Investigation of Brazil Current rings in the confluence region

Carlos A. D. Lentini,[1] Gustavo J. Goni,[2] and Donald B. Olson[3]

[1] TOPEX/Poseidon-derived along track SHA, climatological temperature, and salinity fields were used within a two-layer scheme to estimate the depth of the 8°C isotherm in the southwestern Atlantic. These fields were used to monitor the formation and characteristics of the Brazil Current warm-core anticyclonic rings shed by the first meander trough after poleward excursions of the Brazil Current (BC). Results reveal that 40 warm-core rings were shed by the BC between January 1993 and October 1998. The observed lifetime ranges between 1 and 4 months, with a mean value of approximately 2 months. At any given time, two to three anticyclonic rings coexisted in the Brazil-Malvinas confluence region. Most of the rings drifted southward without coalescing with their parent current. Only four rings were identified as being reabsorbed by the BC front after they were shed. No evidence of propagation or absorption of these anticyclones into the eastern limb of the subtropical gyre was observed. These rings have a mean horizontal length scale of 55 km, mean upper-layer thickness of 260 m, and mean translation speed of 10 km d^{-1}. Volume anomaly and available potential energy computations showed a mean value of 3.6×10^{12} m^3 and 2.5×10^{15} J, respectively. The upper layer transport of the BC was also computed, and a relationship between variations in the southward transport and ring shedding activity was examined. Computation of the heat flux anomaly of the BC rings is estimated to be approximately 0.045 PW per annum. Compilation of these results indicates that warm-core rings created by meandering boundary current extensions in different regions are generally similar.

1. Introduction

[2] The lack of continuous long-term hydrographic observations, specially in the southwestern Atlantic Ocean, makes satellite-derived data an extremely useful tool to investigate time and spatial variability of boundary current systems such as the Brazil-Malvinas Confluence region [*Goni et al.*, 1996, 1997; *Goni and Wainer*, 2001; *Lentini et al.*, 2000, 2001, 2002; *Olson et al.*, 1988; *Vivier and Provost*, 1999]. Unlike infrared imagery, which only reflects the thermal conditions in a very thin layer of the sea surface, altimeter signals are unaffected by cloud coverage and provide information on the vertical thermal and dynamical structure of the upper ocean when complemented by climatological hydrographic data within a diagnostic model [*Goni et al.*, 1996, 1997; *Goni and Wainer*, 2001].

[3] Mesoscale oceanic features, which may be primarily formed by finite-amplitude instabilities of boundary current systems, result in a shedding of a volume of fluid into a region with different environmental characteristics [*Olson*, 1991]. Evidence suggests that temperature and salt anomalies associated with these rings are important sources for water mass modification [*Tomosada*, 1978; *Schmitt and Olson*, 1985; *Gordon*, 1989; *Olson et al.*, 1992] and thermocline ventilation through air-sea interaction in the ring core [*Dewar and Flierl*, 1987; *Olson*, 1991]. Therefore it is clear that the number of rings shed per year by their parent currents and their characteristics may determine how effectively and significantly distinct environments exchange their properties locally. Another important issue is to investigate whether these rings rejoin the boundary current as in the Gulf Stream [*Brown et al.*, 1986] or are completely entrained into another segment of the large-scale circulation as it occurs with Agulhas [*Olson and Evans*, 1986; *Gordon and Haxby*, 1990; *Byrne et al.*, 1995] and Kuroshio rings [*Tomosada*, 1986], or with the East Australian eddies [*Nilsson and Cresswell*, 1981].

[4] In a recent study, *Lentini et al.* [2002] described the statistics of warm-core rings formed in the Brazil-Malvinas Confluence region, where for the first time, a continuous time series of satellite data was used to study the Brazil Current rings. This time series spun from January 1993 to December 1998. These results, which were derived from NOAA polar-orbiter AVHRR 5-day composites, showed that, on average, seven rings per year were released into subantarctic waters. The AVHRR-derived ring lifetime ranged from 11 to 95 days, with a mean value of 35 days,

[1]Instituto Oceanográfico, Universidade de São Paulo, Sao Paulo, Brazil.
[2]Physical Oceanography Division, Atlantic Oceanographic and Meteorological Laboratory, NOAA, U. S. Department of Commerce, Miami, Florida, USA.
[3]Division of Meteorology and Physical Oceanography, Rosenstiel School of Marine and Atmospheric Science, University of Miami, Miami, Florida, USA.

and did not present a bimodal distribution as is the case of Gulf Stream anticyclonic rings [*Brown et al.*, 1986]. After formation, these rings were mostly elliptical anticyclonic rings with a mean major radius of 126 ± 50 km and a minor radius of 65 ± 22 km, and with translation speeds ranging from 4.2 to 27.2 km day^{-1}. None of them seemed to remain more than 4 months in the confluence region.

[5] This work uses the same methodology applied by *Goni and Wainer* [2001] and *Goni et al.* [1996] to compute the upper layer thickness (ULT) fields in the southwestern Atlantic. These ULT fields are used here to investigate the spatial/temporal distribution, trajectory, and speed of translation of a number of warm-core rings formed in the Brazil-Malvinas Confluence region ($60°W–20°W, 30°S–50°S$) shed by the Brazil Current poleward extension. These fields are also used to provide an estimate of the ring volume anomaly and available potential energy content, which may be important in terms of heat and salt transport, at least locally.

[6] Despite the lack of synoptic cruises specifically designed to survey Brazil Current rings, their contribution in terms of heat flux can still be investigated by using remote sensing derived estimates. These estimates are obtained based on a two-layer model, which enables one to relate the depth of a particular isotherm (here the $8°C$ isotherm) to the dynamic height [*Gordon*, 1989; *Olson*, 1991].

[7] The objective of this work is twofold. First, it compares the Brazil Current ring statistics derived from TOPEX/Poseidon (T/P) altimeter with those previously obtained by using infrared data [*Lentini et al.*, 2002]. Second, it provides an estimate of the amount of available potential energy and volume anomaly carried by these anticyclonic rings into subantarctic waters.

[8] This manuscript is outlined as follows. In section 2, computation of the ULT fields and the methodology used to estimate the length scale, volume anomaly and available potential energy of a ring are discussed. In section 3, results and discussion are presented. This section is subdivided into ten subsections. In subsections 1 through 5, the ring identification and its properties (i.e., translation speed, length scale, volume anomaly, and energetics) are discussed. In subsection 6, the statistics obtained from infrared data with those derived from the upper layer thickness fields are compared. In subsection 7, a possible relationship between the Brazil Current southward transport and the ring shedding activity is also investigated. In subsection 8, the T/P ring statistics are compared with those resulting from previous observational studies and from different ocean basins. In subsections 9 and 10, the ring-induced heat flux and the fate of the Brazil Current rings are computed. In section 4, summary and final conclusions are presented.

2. Data and Methods

2.1. Altimeter Data

[9] The T/P-derived sea height anomaly, $\eta'(x, y, t) = \eta(x, y, t) - \overline{\eta}(x, y)$, is the deviation of the actual sea height, η, referred to the mean sea height, $\overline{\eta}$. The mean sea height used in this work, to which the anomalies are computed, are referred to a period of 5 years, 1993 to 1998. The T/P

altimeter measures the sea height anomaly (SHA) along satellite ground tracks, which are approximately separated by 3 degrees longitudinally and repeat every 9.91 days. The data used in this work have the standard altimetric corrections [*Cheney et al.*, 1994] and were interpolated into a 9-km along-track grid for regions deeper than 1000 m. An objective analysis scheme [*Mariano and Brown*, 1992] was used to interpolate the SHA fields into a $0.2°$ by $0.2°$ grid every 10 days, as in work by *Goni et al.* [1996] and *Goni and Wainer* [2001], in the confluence region. Minimum estimation variances of around 0.25 times the field variance occur along the altimeter ground tracks, while maximum estimation variances of around 0.33 times the field variance occur in areas distant from the T/P ground tracks [*Goni et al.*, 1996].

2.2. Climatological Data

[10] Climatological temperature and salinity data [*Conkright et al.*, 1998] are used to compute the mean values of the ULT, which extends from the surface to the depth of the $8°C$ isotherm, and to estimate a mean reduced gravity field for the region of study. *Gordon* [1989] and *Garzoli and Garraffo* [1989] observed a linear relationship between the $8°C$ isotherm and the 0/1500 dynamic height anomaly, with a correlation coefficient of 0.98. According to A. R. Piola (personal communication, 2001), both the $8°C$ and $10°C$ isotherms, which is used by *Goni et al.* [1996], are good proxies to define the South Atlantic thermocline water lower limit in the confluence region. The mean reduced gravity, which provides a measure of the vertical stratification, is given by

$$g'(x,y) = \epsilon(x,y)g(y) = \frac{\rho_2(x,y) - \rho_1(x,y)}{\rho_2(x,y)} g(y), \qquad (1)$$

where g is the acceleration of gravity and ρ_1 and ρ_2 are the mean densities of the upper and lower layers, respectively. The lower layer is defined here as the layer between the depth of the $8°C$ isotherm and 1500 m or the sea floor.

[11] In a baroclinic ocean, changes in thermocline depth are compensated by changes in sea level (Figure 1). Therefore, using a two-layer model approximation, the upper layer thickness, h_1, is given by [*Goni et al.*, 1996],

$$h_1(x,y,t) = \overline{h}_1(x,y) + h_1'(x,y,t)$$
$$= \overline{h}_1(x,y) + \frac{1}{\epsilon(x,y)}[\eta'(x,y,t) + B'(x,y,t)], \qquad (2)$$

where: h_1 is the altimetry-derived upper layer thickness, $\overline{h}_1$ is the climatological derived mean ULT, h_1' is the ULT anomaly, and B' includes the barotropic contribution to the sea height anomaly. The values of ULT associated with an anticyclonic ring will increase as the ring center approaches the satellite ground track.

[12] Hydrographic casts yield only the baroclinic sea level component, while satellite altimetry observes the combined barotropic and baroclinic sea level components. As shown by *Mellor et al.* [1982] in a numerical model study of the Atlantic Ocean, the barotropic component can be smaller than the baroclinic counterpart or even insignificant in some areas of non-prominent bottom topography or
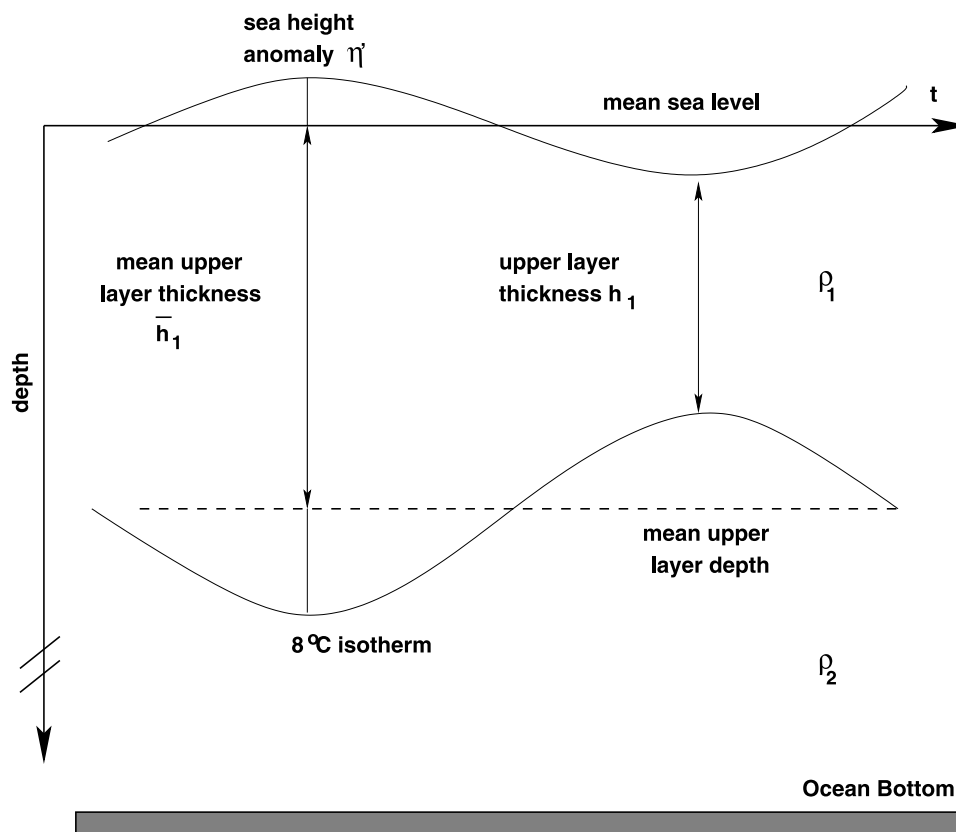
Figure 1. Schematic representation of the upper ocean dynamics in a two-layer reduced gravity scheme, where η' is the sea height anomaly, h_1 is the upper layer thickness, and ρ_1 and ρ_2 are the mean water densities of the upper and lower layers, respectively.

in regions where baroclinic currents are extremely strong. The barotropic contribution to the sea height anomaly is large in the Malvinas Current (MC), whereas it has been shown to be much smaller in the Brazil Current region [*Goni et al.*, 1996]. Therefore the barotropic term is disregarded in this study as it was in work by *Goni and Wainer* [2001]. Although rings typically have a significant barotropic component at their core, this component leads to negligible errors in the integrated estimates of the properties of the rings computed here [*Olson*, 1991].

[13] From the combination of climatological and altimetric data in a two-layer scheme, a total of 210 altimetry-derived ULT fields were obtained and used to identify and investigate the Brazil warm-core rings and their trajectories in the confluence region during the period from January 1993 to October 1998. As an example, the SHA field for 27 February 1995 and its corresponding ULT field are shown in Figure 2, before the shedding of a Brazil Current ring. The thick white line in the ULT map (bottom panel) shows the location of the 8°C isotherm estimated using (2) at ∼200 m depth, which has been defined as the location of the Brazil Front [*Garzoli and Garraffo*, 1989; *Garzoli and Bianchi*, 1987; *Goni and Wainer*, 2001]. Anticyclonic rings are identified here as regions of closed ULT contours that have length scales larger than 0.2 degrees latitude/longitude and with increasing ULT toward their centers. Their locations, estimated with an error not larger than 1/4

of a degree [*Goni et al.*, 1997], are placed at the point of maximum ULT.

[14] Despite the advantages of using satellite altimetry in this region, some uncertainties on the ring identification can be raised. For example, the T/P altimeter sensor cannot identify an isolated feature (ring) when it is inside the diamond-shaped grid formed by the intersection of contiguous ascending and descending ground tracks. A slow-moving small ring may easily "vanish" for a short period of time as it drifts between the T/P ground tracks, leading to discontinuity in the ring-tracking process. Therefore rings that cross one or more ground tracks can be better identified.

2.3. Length Scales

[15] In this study, rings are assumed to have a radial Gaussian upper layer thickness cross-section h_1. Therefore

$$h_1(r) - h_\infty = h_0 e^{-r^2/2L^2}, \qquad (3)$$

where r is the along-track distance measured from the center of the ring, h_1 is the along-track depth of the 8°C isotherm across the ring, h_∞ is the depth of the 8°C isotherm far from the ring, L is the length scale of the ring, which also corresponds to the radius of maximum velocity [*Duncombe Rae et al.*, 1996], and h_0 is the maximum along-track depth of the ring measured from h_∞. The shape of h_1 (ULT) is represented by the radial distribution of the 8°C isotherm to
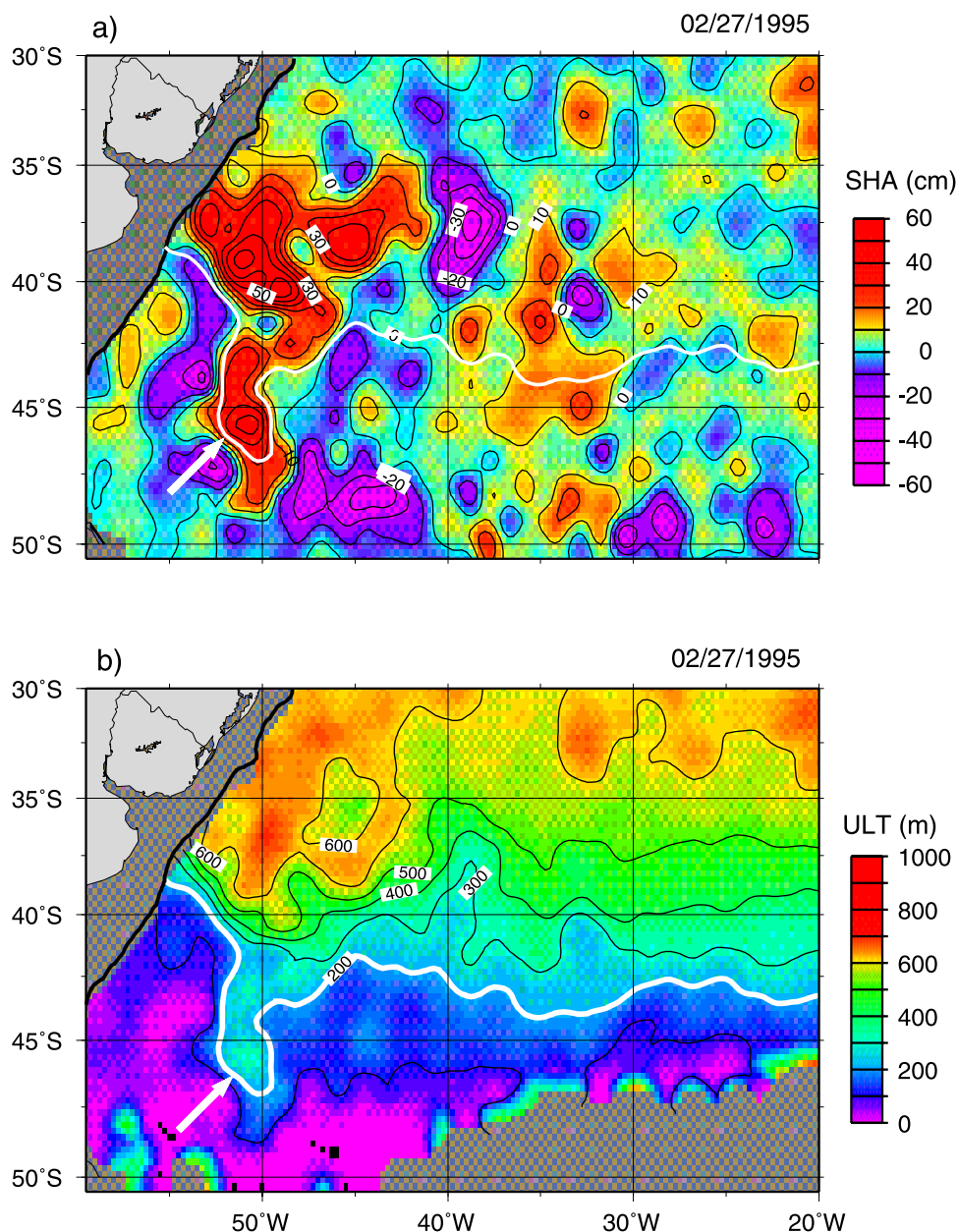
Figure 2. (a) Sea height anomaly (SHA) field for 27 February 1995 and (b) the corresponding upper layer thickness (ULT) field for the same date, before the shedding of an anticyclonic Brazil Current ring indicated by white arrows. The thick white line corresponds to the 200-m ULT contour and the continental shelf break (depths <200 m) off South America is in dark gray.

which a Gaussian function is then fitted. This computation assumes that a T/P ground track crosses the ring through its center.

2.4. Volume Anomaly

[16] The volume anomaly is estimated here to investigate the excess amount of water that an anticyclone introduces into a region of different environmental characteristics [Olson, 1991]. The size of a ring can be quantified in terms of ring volume anomaly [Olson, 1991; Goni et al., 1997], which is that part of the ring volume with waters warmer than 8°C relative to h_∞ [Olson and Evans, 1986]. If an anticyclonic ring is assumed to have a radial Gaussian upper layer thickness

cross-section h_1, then an applicable measure of volume anomaly, VOL, is [Goni et al., 1997],

$$VOL = 2\pi L^2 h_0. \quad (4)$$

2.5. Energetics

[17] The intensity of a ring can be quantified in terms of ring energy content as available potential energy (APE), which is proportional to the part of the potential energy that can be converted into kinetic energy, and is defined as [Olson, 1991]

$$APE = \frac{1}{2}\rho_1 g' \int_A (h_1(r) - h_\infty)^2 dA, \quad (5)$$

Table 1. Brazil Current Ring Statistics Derived From Altimetry[a]

Ring	Month of First Observation	SHA, cm	h_0, m	h_∞, m	h_1, m	L, km	VOL, $10^{12}m^3$	APE, 10^{15}J	V_{mean}, km/d	T, days	rms, m
TP-1-93	Jan 1993	20	17	85	101	45	0.2	0.01	5.8	40	6
TP-2-93	March 1993	40	136	120	256	60	3.1	1.4	6.2	70	27
TP-3-93[b]	May 1993	50	288	50	338	60	6.8	6.3	12.0	40	36
TP-4-93	July 1993	20	85	200	285	30	0.4	0.2	11.6	40	9
TP-5-93[b]	Aug 1993	30	166	70	236	100	10.4	6.2	5.7	50	20
TP-6-93	Aug 1993	20	88	140	228	30	0.5	0.2	12.2	70	5
TP-7-93	Oct 1993	40	129	100	229	45	1.7	0.8	12.3	50	7
TP-8-93	Nov 1993	30	85	130	215	65	2.3	0.7	6.6	120	16
TP-9-94[c]	Jan 1994	40	200	120	320	45	2.6	1.8	11.1	70	27
TP-10-94	Feb 1994	40	240	30	270	45	3.1	2.7	2.7	30	23
TP-11-94[b]	May 1994	40	249	30	279	70	7.7	6.9	6.5	40	25
TP-12-94	July 1994	20	81	140	221	70	2.5	0.7	5.4	80	12
TP-13-94[b]	Oct 1994	30	200	30	230	90	10.2	7.3	4.7	60	11
TP-14-94	Dec 1994	20	47	140	187	65	1.3	0.2	12.0	30	10
TP-15-95	Jan 1995	20	114	80	194	45	1.5	0.6	8.5	90	9
TP-16-95	Jan 1995	20	151	60	211	35	1.2	0.6	6.5	40	19
TP-17-95	March 1995	40	152	90	212	60	3.4	1.9	13.1	60	9
TP-18-95	June 1995	30	101	160	261	55	1.9	0.7	11.7	30	8
TP-19-95[b]	July 1995	40	223	120	343	60	5.1	4.1	8.5	40	36
TP-20-95[b]	Aug 1995	40	227	30	257	60	5.1	4.2	9.0	50	21
TP-21-95[c]	Sep 1995	30	108	160	268	40	1.1	0.4	15.1	30	6
TP-22-95[b]	Oct 1995	40	218	40	258	70	6.7	5.2	6.2	50	36
TP-23-95	Nov 1995	30	122	100	222	50	1.9	0.8	22.8	40	28
TP-24-95	Dec 1995	30	208	120	328	50	3.3	2.4	9.2	50	23
TP-25-96	Jan 1996	20	114	80	194	40	1.2	0.5	17.2	90	9
TP-26-96	Feb 1996	30	204	45	249	50	3.2	2.4	10.9	50	17
TP-27-96	April 1996	30	147	120	267	55	2.8	1.5	4.2	60	16
TP-28-96[b, c]	May 1996	50	288	30	318	55	5.5	5.7	6.7	50	23
TP-29-96[b]	June 1996	40	147	110	257	75	5.2	2.7	6.7	100	14
TP-30-96	Sep 1996	30	156	150	306	35	1.2	0.7	14.9	60	13
TP-31-96	Dec 1996	40	158	150	308	40	1.6	0.9	10.4	40	29
TP-32-97	Feb 1997	20	166	80	236	40	1.7	1.0	17.4	30	9
TP-33-97	June 1997	20	141	100	241	55	2.7	1.4	14.5	20	13
TP-34-97[b]	Sep 1997	50	309	30	339	65	8.2	9.1	8.1	100	33
TP-35-97	Dec 1997	20	87	130	217	45	1.1	0.3	1.3	30	16
TP-36-98	Feb 1998	20	116	120	236	60	2.6	1.1	8.8	40	13
TP-37-98[b]	April 1998	30	212	40	252	90	10.8	8.2	10.3	30	39
TP-38-98	June 1998	40	135	200	335	50	2.1	1.0	10.9	70	16
TP-39-98[b]	July 1998	30	215	80	295	60	4.9	3.7	2.4	40	34
TP-40-98[b, c]	Sep 1998	20	217	50	267	55	4.1	3.2	14.4	40	12
Average		30	161	97	257	55	3.6	2.5	9.8	53	18

[a]The name of each ring indicates the year and order it was shed. The second column indicates the month and year when the rings were first detected from the altimeter data; SHA is the maximum along-track sea height anomaly; h_0 is the maximum upper layer thickness obtained from the Gaussian fit, relative to the upper layer thickness of the waters surrounding the ring; h_∞; $h_1 = h_0 + h_\infty$ is the upper layer thickness; L is the radius of maximum velocity; VOL is the volume anomaly; APE is the available potential energy; V_{mean} is the mean translation speed; T is the lifetime; and rms, in the last column, is the root-mean-square error for the least-squares nonlinear fit to a Gaussian function.

[b]These are considered relatively large rings ($VOL > VOL_{mean}$).

[c]These are reabsorbed rings. Ring TP-21-95 corresponds to Ring Leon, which after three T/P cycles (~30 days) is reabsorbed by the Brazil Current front.

where ρ_1 is the mean density of the upper layer, g' is the reduced gravity, A is integral of the area occupied by the ring, and r is the radius of the ring. For an anticyclonic ring with a radial Gaussian upper layer thickness cross-section h_1, the available potential energy is given by [*Goni et al.*, 1997]

$$APE = \frac{\pi}{2} \rho_1 g' h_0^2 L^2. \qquad (6)$$

3. Results and Discussion

[18] All rings identified were also tracked along their paths until they could no longer be distinguished from the ULT fields. The notation applied here to name each ring uses the letter "TP" followed by two numbers indicating the order and the year in which the ring is first observed. For instance, ring "TP-5-93" is the fifth ring identified as having been formed during 1993. Ring parameters are computed following the methodology described above.

3.1. Ring Identification

[19] A total of 40 anticyclonic rings are identified using the criteria described in section 2.2 (Table 1). The average number of rings formed per year is 6.6, with a marked decrease in ring formation beginning in 1996, reaching a minimum number during 1997 (Figure 3).

[20] The trajectories of the 40 Brazil Current rings formed during the period of study are shown in Figure 4. The squares (triangles) indicate the locations where the rings are first (last) identified from the ULT fields. Although ring trajectories differ from year to year suggesting the existence of marked interannual variability, they appear to be confined

	Jan	Feb	Mar	Apr	May	Jun	Jul	Aug	Sep	Oct	Nov	Dec	Per Year
1993	●		●		●		●	● ●		●	●		8
1994	●	●			●		●			●		●	6
1995	● ●		●			●	●	●	●	●	●	●	10
1996	●	●		●	●	●			●			●	7
1997		●				●			●			●	4
1998		●		●			●	●		●	▨	▨	5
Summary	5	4	2	2	3	3	4	4	3	4	2	4	40

No data = ▨
Ring = ●

Figure 3. Formation times of Brazil Current rings, where black circles indicate the time when Brazil Current rings were shed. Squares indicate times when no sufficient data were available to correctly identify a ring.

to a limited region between 41°S and 49°S, and from 58°W to 40°W (Figure 5), and to have different directions of propagation. The root-mean square (rms) values of the SHA field in the same region indicate that the largest values of RMS are associated to the motion of the Brazil Current front and not to the translation of Brazil Current rings (Figure 5). Almost half of the total of the rings (19 rings) show a general tendency to propagate in a SW direction across the region, ten rings follow a SE direction, and only three rings are observed to follow a NE direction. The remaining anticyclones (8 rings) propagate in a NW direction. Within this last subset, only four rings are reabsorbed by the Brazil Current (Table 1), whereas the other seven rings seem to disappear in the confluence region without rejoining their parent current. Although their sea surface temperature signature may dissipate owing to the atmospheric cooling in winter and/or owing to interactions with the cold Malvinas Current, we have not yet attempted to address these issues. It is observed that none of the rings remain in the region for more than 4 months, nor cross the 1000-m isobath. Moreover, no evidence of propagation or absorption of Brazil Current rings into the eastern limb of the subtropical gyre is observed, as previously reported by *Smythe-Wright et al.* [1996]. This result is supported by the work of *McDonagh and Heywood* [1999], who proved that the ring described by *Smythe-Wright et al.* [1996] is in fact a subsurface Agulhas ring moving into the eastern part of the subtropical gyre.

[21] The lifetime of a ring, defined here as the period of time a ring can be detected from the ULT fields, is computed for each ring in the region of study between January 1993 and October 1998. Residence time for each ring is shown in the eleventh column of Table 1. The observed ring lifetimes range from 20 days to 120 days, with a mean value of 53 days. Rings with the longest lifetimes are TP-8-93, TP-29-96 and TP-34-97 with 120, 100, and 100 days, respectively. For example, ring TP-8-93 was formed at the end of 1993 and remained in the region for 4 months, lasting almost until the end of austral summer of 1994.

3.2. Translational Velocity

[22] The mean translation velocity is estimated using the ULT fields by computing the ratio between integrated track length and the lifetime of each ring. This velocity is a combination of the beta-induced ring motion with its advective velocity component due to the large-scale mean circulation, and with its motion due to interaction with boundary currents.

[23] After being shed, rings generally translate southward with motions ranging from 1.3 to 22.8 km d^{-1}, and a mean translation speed of 9.8 ± 4.7 km d^{-1} (see Table 1). Top speeds of about 20–23 km d^{-1} correspond to rings TP-21-95 and TP-23-95, whereas the lowest mean translation speed of 1.3 km d^{-1} corresponds to ring TP-35-97. According to *Legeckis and Gordon*'s [1982] infrared observations, the Brazil Current rings move southward from the subtropical zone into the subpolar gyre at an average translation speed of approximately 25 km d^{-1}. Another indication of the relatively high translation speed of these rings is given by *Figueroa et al.* [1998]. Using this mean velocity value, the authors were able to explain the occurrence of tropical-subtropical species of mesopelagic fish farther south in subantarctic waters at approximately 53°S and 60°W. These thermophilic species, trapped inside an anticyclonic Brazil Current ring, are transported southward out of the
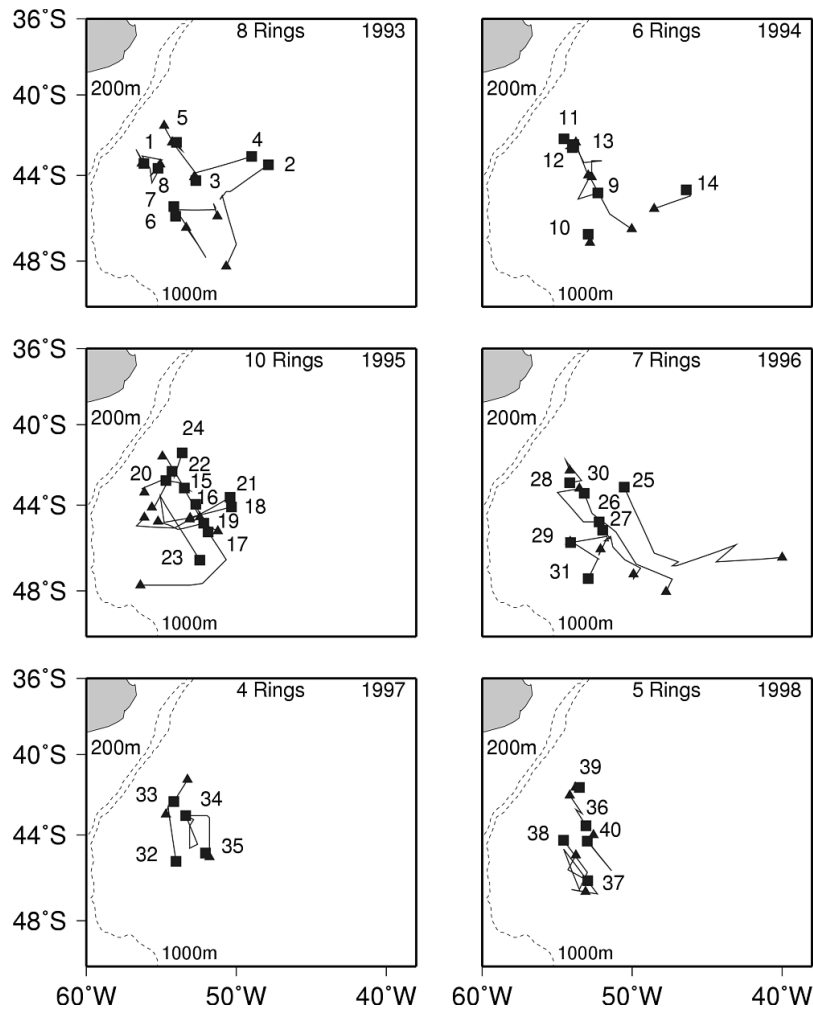
Figure 4. Trajectories of the Brazil Current rings formed between January 1993 and October 1998. The squares indicate the location where the warm rings are first observed, whereas the triangles indicate the point at which they can no longer be tracked using the ULT fields. None of the rings were observed to translate east of 40°W.
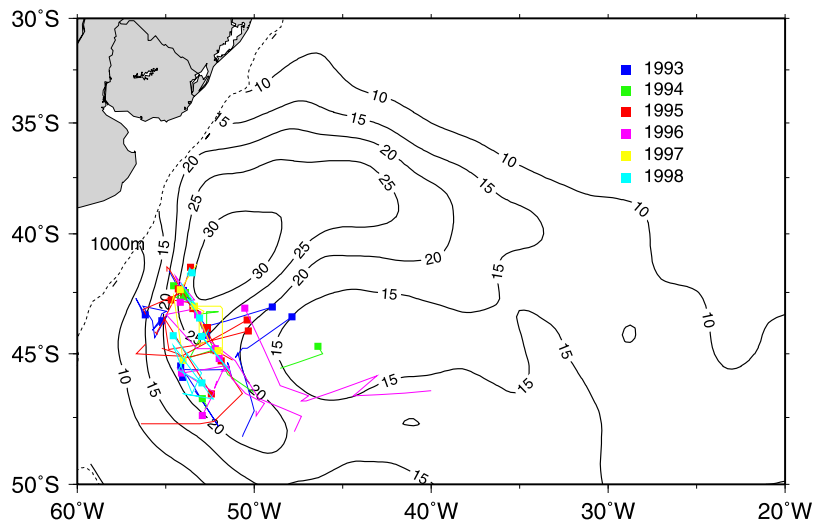
Figure 5. Brazil Current ring trajectories superimposed to the root-mean square (rms) sea height variability derived from T/P data. The ring trajectories appear to be confined to a region limited by 36°S and 49°S, and from 40°W to 58°W. The 1000-m isobath is also superimposed to the map.
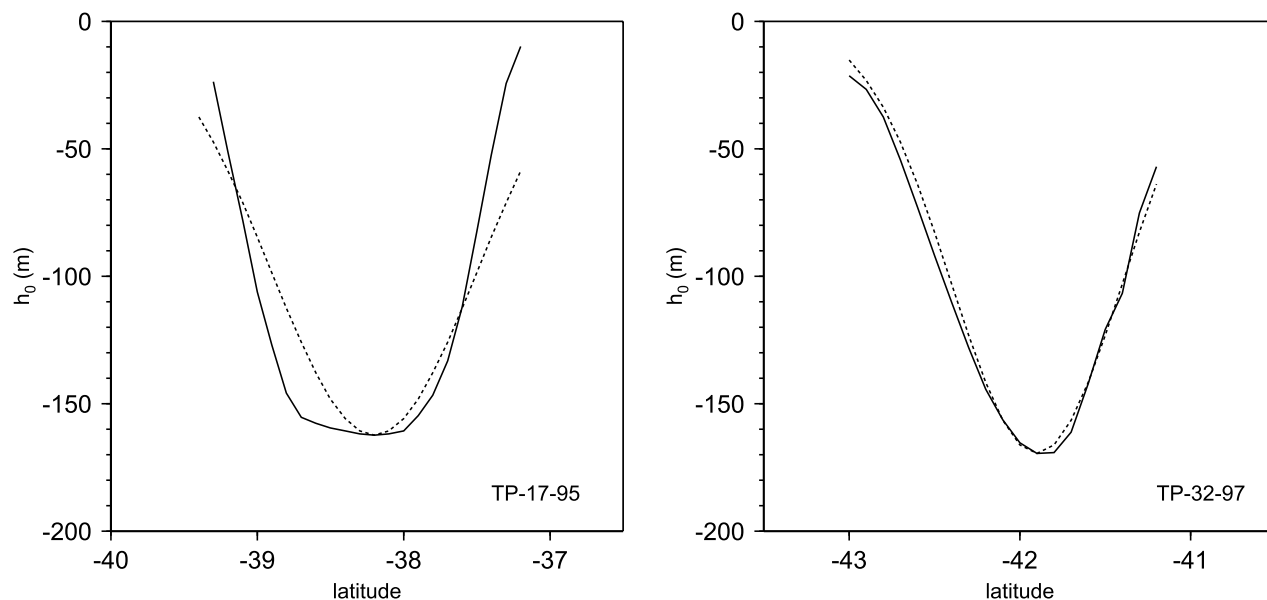
Figure 6. Least squares nonlinear fit of a Gaussian function (equation (3)) to the altimeter along-track upper layer thickness values for rings TP-17-95 (left panel) and TP-32-97 (right panel). The solid line is the maximum along-track depth h_0 referenced to h_∞, and the dashed line is the estimated ring cross section obtained using the nonlinear fit.

subtropical zone into the subantarctic regime. According to *Figueroa et al.* [1998], the population persists as long as the ring maintains its physical properties.

[24] The influence of the large-scale flow in the advection of the Brazil Current rings has been estimated assuming a two-layer ocean with upper layer (250 m deep) density $\rho_1 = 1.0265 \text{ g/cm}^3$ and lower layer density $\rho_2 = 1.0280 \text{ g/cm}^3$, at approximately 40°S. The computed first baroclinic radius of deformation R_d is 19 km, which falls within the range of R_d values (20–30 km) that are representative of the confluence region [*Forbes et al.*, 1993; *Houry et al.*, 1987]. According to *Nof*'s [1981] and *Flierl*'s [1984] theories, long baroclinic Rossby wave speeds, which are proportional to βR_d^2, propagate westward toward the western boundary current at speeds of approximately 3 km d^{-1}. However, this speed is slower than the average translation speed of 9.8 km d^{-1} as for the T/P-derived Brazil Current rings, suggesting that advection by the large-scale flow exerts only a weak-to-moderate influence on the propagation of a ring.

3.3. Length Scales

[25] The parameters h_0, h_∞, and L are estimated along the altimeter ground track by fitting (3) with a least squares method to the ULT cross section when the rings are first detected on the ULT fields. This least squares nonlinear fit to the Gaussian function (3) is then performed by allowing L span a range of values between 10 and 250 km at intervals of 5 km in a similar approach that has been previously applied on North Brazil Current rings [*Didden and Schott*, 1993] and Agulhas rings [*Goni et al.*, 1997]. An example of the fitting of (3) to two Brazil Current rings (rings TP-17-95 and TP-32-97) is shown in Figure 6. The *rms* error estimates for the nonlinear fit of the 40 Brazil Current rings range from approximately 5 to 40 m (last column in Table 1).

[26] The mean maximum depth value of all surveyed Brazil Current rings ($h_1 = h_0 + h_\infty$) is 256.8 ± 50.3 m. Rings

TP-3-93, TP-19-95, TP-34-97, and TP-38-98 have the largest ULT values, reaching depths of approximately 340 m. The mean value of the length scale, L, for all the observed rings is 55.4 ± 15.8 km. The largest values of L, of 100 km, corresponds to ring TP-5-93, which can be tracked for almost 2 months before it can no longer be detected from the ULT fields.

[27] The uncertainty in the estimates of L depends on the least squares nonlinear fit of the radial shape of h_1, on the section of the ring being crossed by the satellite ground track when it is first observed, and on the fact that the ring is not symmetrical. Values of RMS errors included in the last column of Table 1 indicate that the Gaussian fit performs quite well, with a mean RMS error of 18 m. When the satellite ground track crosses the center of a ring, the altimeter observed SHA and derived ULT values are closer to their actual values. However, as the ring translates, it is expected that different parts of the ring will be juxtaposed onto the T/P ground tracks, producing a reduction of 10–30% in the values of L. Therefore, at any given time, the actual size of the ring is probably being underestimated. However, assuming that rings are symmetrical, instead of elliptical, and that the T/P ground tracks cross the rings through their centers, the computed ring dimensions do not seem to give unreasonable values of L when compared to the results of previous observational studies [*Legeckis and Gordon*, 1982; *Gordon*, 1989; *Figueroa et al.*, 1998; *Vigan et al.*, 2000; *Lentini et al.*, 2002].

3.4. Volume Anomaly

[28] The values of h_0, h_∞, L, and *VOL* of each of the forty Brazil Current rings are shown in Table 1. The values of *VOL* range from $0.2 \times 10^{12} \text{m}^3$ to $10.8 \times 10^{12} \text{m}^3$. Within any given year, at least one "large" Brazil Current ring, with *VOL* larger than the mean (i.e., $3.6 \times 10^{12} \text{m}^3$), is released into subpolar regions (see Table 1, rings marked
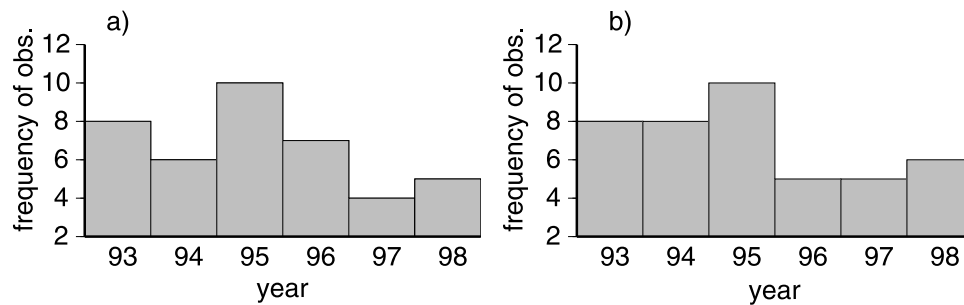
Figure 7. Ring distribution frequency histogram obtained from (a) the altimetry-derived upper layer thickness method and (b) the AVHRR-derived sea surface temperature observations. The mean number of rings shed per year is ~7. A clear decrease in ring shedding activity is observed beginning in 1996.

with an "a"). As expected, these rings also correspond to horizontal scales greater than the average horizontal scale L and h_0 depths of at least 150 m. Assuming $L = 55$ km and $h_0 = 160$ m as mean values for a typical Brazil Current ring, the volume anomaly amounts to $3 \times 10^{12}\,\text{m}^3$. Based on in-situ observations by Gordon [1989], computations of volume anomaly for rings Anthony and Asp give VOL values of 3.8 and 6.2 $\times 10^{12}\,\text{m}^3$, respectively. These volume anomalies were calculated using values of L of 55 km and 70 km, and $h_0 = 200$ m [Gordon, 1989, Figure 15]. Table 1 shows that the VOL values for the entire ring population are in good agreement with computations based on in situ observations.

3.5. Energetics

[29] Estimated values of APE for each of the 40 Brazil Current rings are shown in Table 1. Initial APE values for the entire ensemble range from values as low as $0.01 \times 10^{15}\,\text{J}$ to $9.1 \times 10^{15}\,\text{J}$, with a mean APE of $2.5 \times 10^{15}\,\text{J}$. The APE estimates are compared with in situ observations [Gordon, 1989] and used to obtain a ring decay scale [Okada and Sugimori, 1986; Olson et al., 1985; Olson, 1991]. A possible interpretation for some of the low values of available potential energy (Table 1) can be associated with the determination of the parameters of a ring when it is first detected from the ULT fields. Estimation of available potential energy is considerably more sensitive than the volume anomaly estimates, because both L and h_0 in (6) are quadratic in the APE expression (6) but linear in VOL (4). Moreover, the parameter h_0, which is the maximum along-track depth of the ring measured from h_∞ (Figure 1), is also dependent on the distance of the center of the ring to the T/P ground track. Although the ring location estimates have errors not larger than 1/4 of a degree when the rings are first observed, the discrepancies in APE suggest that the assumption that T/P ground tracks cross the rings through their centers may not be the best approach. Calculations of energy content for rings Asp and Anthony [Gordon, 1989] gave values of approximately 2.0 and 9.0×10^{15} J, respectively [after Olson, 1991]. Nevertheless, APE computations are consistent and have the same order of magnitude as those calculated for these two mesoscale features through direct observations.

[30] The decay rate of APE ranges from -0.9×10^8 to -3.0×10^8 W day^{-1} [Olson, 1991] when rings are outside the influence of major currents and when they are also dependent on the reference level used to define the interface between layers. An initial mean APE content of 2.5×10^{15} J for the entire subset of Brazil Current rings suggests a decay timescale (APE divided by its decay rate) that ranges between 96 and 322 days when a ring is outside the influence of a major current. Calculations of energy content for rings Asp and Anthony [Gordon, 1989] suggest a decay timescale of 80 days to 3.2 years, respectively. In fact, the decay timescale for ring Anthony could have been overestimated either by not considering the influence of the two opposing currents and interactions with other rings, or by not taking into account the small-scale lateral mixing.

[31] While the investigation of the influence of boundary currents on physical properties of a ring, ring-to-ring interactions, and generation of ring-induced streamers is not within the scope of this work, we can at least speculate on the small-scale mixing influence. Lateral mixing can be also considered as a potential mechanism for the dissipation of rings [Mied, 1989; Olson, 1986, 1991] that are shed from the southern excursions of the Brazil Current. Given the temperature flux (which is proportional to the heat flux if multiplied by ρ Cp) calculated for the Brazil-Malvinas confluence as 1.2×10^{-2} °C m s^{-1} [Bianchi et al., 1993], a 250 m deep and 110-km-wide ring with a temperature anomaly of ~5°C [Lentini et al., 2002] would dissipate in approximately 4 months. This estimate should not be interpreted as the mean lifetime of a ring, but rather as an indication that the small scale lateral mixing can be relatively important in terms of thermal dissipation of the Brazil Current rings.

3.6. Comparison Between Altimetry and AVHRR Results

[32] Owing to the scarcity of direct hydrographic observations of mesoscale features in the confluence region, Leon (here TP-21-95) is the only anticyclonic ring documented in the literature [Hooker and Brown, 1996; Vigan et al., 2000] within the 6-year time frame of this study.

[33] A total of 426 5-day composites (January 1993 to October 1998) produced at RSMAS (University of Miami) were used to validate the location, size and mean lifetime of the T/P-derived rings. The reader is referred to Lentini et al. [2002] for a full statistics of AVHRR-derived Brazil Current rings.

[34] A comparison between ULT and SST-derived Brazil Current rings is shown in Figures 7, 8, and 9. Table 2
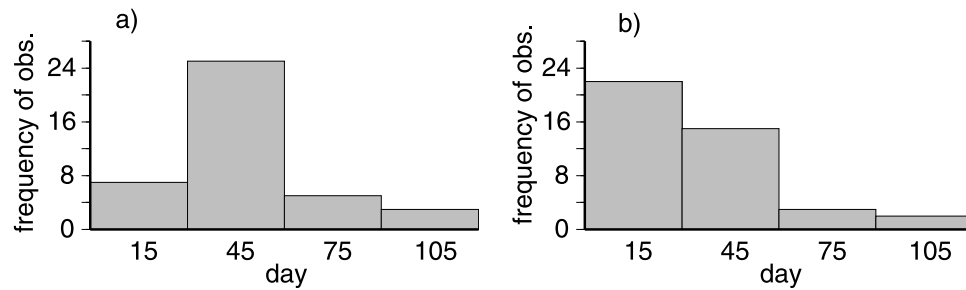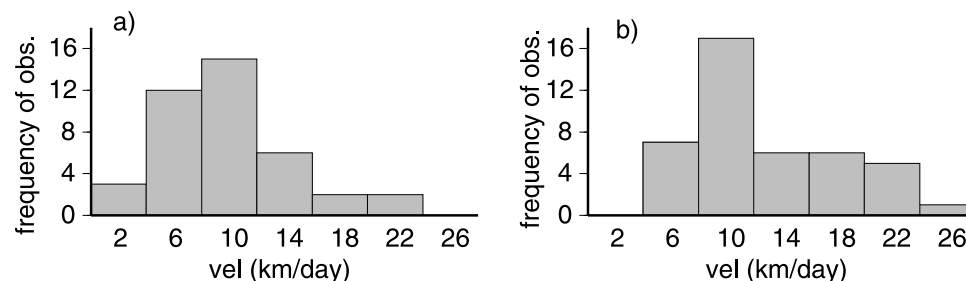
Figure 8. Ring lifetime frequency histogram obtained from (a) the altimetry-derived upper layer thickness method, and (b) the AVHRR-derived sea surface temperature observations. The mean lifetime is 53 days in Figure 8a and 35 days in Figure 8b.

indicates rings that are observed using AVHRR and altimetry. The term "AV" in Table 2 stands for "AVHRR observations" followed by its corresponding number in the TP statistics (see Table 1) and the year. For example, ring AV-4-93 corresponds to ring TP-4-93. AVHRR rings that were not observed simultaneously on the ULT fields have no ring number, only the year of observation.

[35] According to Figures 7, 8, and 9 and to Table 2, the overall statistics are very similar and a significant percentage (~75%) of ULT-derived Brazil Current rings is also observed in the SST surface fields. Although the ULT-derived length scale (L) and translation velocity of these rings are most likely to be underestimated, comparisons between the ULT-derived and SST observed rings are encouraging, and the ULT-derived method used here appears to be a reasonable approach in regions historically undersampled by conventional platforms such as ships and buoy observations. For example, the ULT-derived L for ring TP-21-95 is 40 km, half the size of the value reported by *Vigan et al.* [2000] and derived from the AVHRR 5-day composites (see Table 2). This difference, which accounts for 50% of the horizontal length scale of the ring, may be due to the different definition of length scale. From hydrographic observations, the value of L is determined at the level of the strongest vertical shear of swirl velocities [*Joyce and Kennelly*, 1985; *Olson et al.*, 1985; *Fratantoni et al.*, 1995]. However, in studies that use infrared observations, the maximum swirl velocity does not coincide with the strongest surface thermal gradient, but rather inside it [*Vigan et al.*, 2000]. It is very reasonable to assume that this fact accounts for the difference in the computed radius (length scale) between Leon and TP-21-95. Ring Leon, which was

shed by the Brazil Current approximately on 20 September 1995, moved northwestward and was reabsorbed by the Brazil-Malvinas front after only 2 weeks. The difference between the ULT-derived and SST-derived lifetime is ~20 days. The mean lifetime for altimetry- and AVHRR-derived rings are 53 and 35 days, respectively. We speculate that the longer lifetime observed with altimetry is due because in many instances the sea surface temperature signal of a ring erodes before its sea height signal does, particularly during the winter months.

[36] A correspondence between the sea surface temperature and the sea height anomaly fields does not always exist, and when it does, it may have strong geographical and seasonal components related to the physical processes affecting, for example, the ocean dynamics and surface fluxes [*Vukovich and Maul*, 1985]. An example is presented here for two Brazil Current rings, rings TP-17-95 and TP-39-98, where the sea height anomaly and sea surface temperature fields are shown for each ring (Figures 10 and 11). The sea height anomaly field for Ring TP-17-95 (Figure 10) corresponding to 22 March 1995, shows maximum values reaching approximately 40 cm in the ascending (descending) T/P ground track at 52°W, reaching values of 60 cm above the surrounding waters. The correspondent ULT field (not shown here) indicates that this feature corresponds to a ring detached from the Brazil Current and not to an extreme southern excursion of the Brazil Current front. The sea surface temperature field corresponding to 19 March 1995 shows that this ring has a weak thermal signal of approximately 14.5°C. The sea height anomaly obtained during 22 July 1998, shows a maximum value of 45 cm named Ring TP-39-98 (Figure 11) and roughly centered at

Figure 9. Ring velocity frequency histogram obtained from (a) the altimetry-derived upper layer thickness method and (b) the AVHRR-derived sea surface temperature observations. Both histogram distributions are skewed toward velocities lower than 12 km/d.

Table 2. Comparison Between Altimetry-Derived Brazil Current Rings and AVHRR-5-Day Composite Observations[a]

| Ring	Month of First Observation	LM, km	Lm, km	L_{mean}, km	ΔT, °C	V_{mean}, km d^{-1}	T, days
AV_1_93	**Jan 1993**	**59**	**44**	**51**	**3.6**	**11.2**	**36**
AV_93[b]	Feb 1993	96	66	81	3.7	13.2	30
AV_2_93	**Feb 1993**	**99**	**65**	**82**	**2.9**	**22.8**	**38**
AV_3_93	**May 1993**	**90**	**80**	**85**	**6.8**	**14.8**	**45**
AV_4_93	**July 1993**	**67**	**60**	**63**	**5.0**	**7.9**	**23**
AV_5_93[c]	**Sep 1993**	**165**	**60**	**112**	**6.5**	**19.1**	**35**
AV_7_93	**Oct 1993**	**79**	**70**	**70**	**3.6**	**10.2**	**30**
AV_93	Dec 1993	80	78	79	5.0	6.7	36
AV_9_94[b]	**Jan 1994**	**106**	**47**	**76**	**4.5**	**22.3**	**21**
AV_10_94	**Feb 1994**	**111**	**63**	**87**	**6.0**	**10.7**	**23**
AV_94[c]	April 1994	179	104	141	6.0	21.0	15
AV_11_94[c]	**May 1994**	**154**	**77**	**116**	**6.5**	**11.0**	**30**
AV_94[c]	June 1994	174	77	125	6.3	7.0	30
AV_13_94[c]	**Oct 1994**	**193**	**107**	**150**	**6.8**	**9.1**	**31**
AV_94	Nov 1994	134	43	88	6.3	15.8	20
AV_14_94[c]	**Dec 1994**	**130**	**101**	**116**	**5.1**	**11.3**	**17**
AV_15_95	**Jan 1995**	**78**	**62**	**70**	**4.4**	**7.3**	**36**
AV_17_95	**Feb 1995**	**106**	**65**	**86**	**2.3**	**20.1**	**44**
AV_95	March 1995	94	38	66	6.0	17.0	11
AV_18_95[c]	**June 1995**	**185**	**46**	**115**	**5.8**	**14.5**	**25**
AV_19_95[c]	**July 1995**	**189**	**108**	**149**	**5.0**	**23.9**	**36**
AV_20_95[c]	**Aug 1995**	**102**	**86**	**94**	**6.1**	**19.3**	**41**
AV_21_95[b]	**Sep 1995**	**90**	**73**	**81**	**6.3**	**10.0**	**10**
AV_22_95[c]	**Oct 1995**	**226**	**95**	**161**	**6.3**	**17.9**	**26**
AV_23_95	**Nov 1995**	**56**	**50**	**53**	**5.1**	**13.1**	**20**
AV_24_95[c]	**Dec 1995**	**172**	**44**	**108**	**3.1**	**27.1**	**20**
AV_25_96[c]	**Jan 1996**	**135**	**55**	**94**	**4.3**	**17.0**	**95**
AV_27_96	**April 1996**	**63**	**48**	**55**	**2.9**	**4.2**	**71**
AV_28_96[b, c]	**May 1996**	**109**	**97**	**103**	**6.6**	**6.0**	**31**
AV_30_96[c]	**Sep 1996**	**221**	**39**	**130**	**6.5**	**11.2**	**65**
AV_31_96[c]	**Dec 1996**	**206**	**69**	**138**	**4.0**	**9.7**	**26**
AV_32_97	**Feb 1997**	**98**	**82**	**90**	**4.0**	**9.6**	**23**
AV_97[b]	April 1997	187	30	108	6.4	10.0	19
AV_97	July 1997	82	51	66	6.0	8.7	45
AV_34_97[c]	**Sep 1997**	**201**	**77**	**139**	**6.5**	**8.5**	**91**
AV_97[b]	Nov 1997	68	42	55	3.4	14.9	30
AV_98	Jan 1998	61	37	49	4.6	9.6	59
AV_36_98	**Feb 1998**	**91**	**83**	**87**	**4.8**	**9.8**	**42**
AV_37_98	**April 1998**	**123**	**23**	**72**	**4.8**	**19.7**	**15**
AV_39_98[c]	**July 1998**	**190**	**76**	**133**	**5.4**	**5.8**	**30**
AV_98	Aug 1998	132	73	58	4.2	10.3	36
AV_40_98[b]	**Oct 1998**	**111**	**37**	**74**	**5.9**	**10.0**	**71**
Average		**126**	**65**	**94**	**5.1**	**13.1**	**35**

[a]Thirty-one (bold) out of forty-two rings are simultaneously observed. LM is the major semi-axis, Lm is the minor semi-axis, L_{mean} is the mean semi-axis, ΔT is the temperature difference between the inner core of a ring and the surface temperature of the surrounding waters outside its influence, and V_{mean} is the mean translation speed.

[b]These are recoalesced rings.

[c]These are relatively large ($L > L_{mean}$) rings.
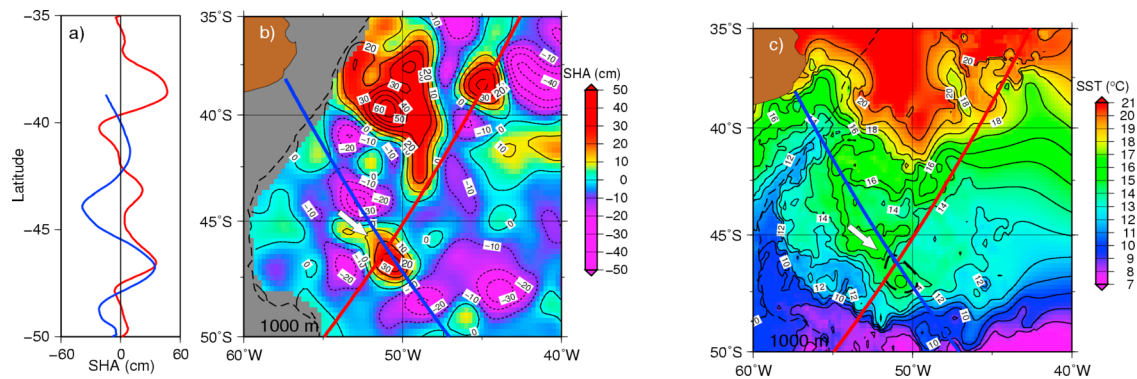
Figure 10. (a) Along-track sea height anomaly (SHA) of ring TP-17-95 on 22 March 1995 for two altimeter ground tracks, (b) SHA field on the same date, and (c) sea surface temperature (SST) field on 19 March 1995. The arrows indicate the location of a Brazil Current ring. The two altimeter ground tracks are superimposed to the maps.
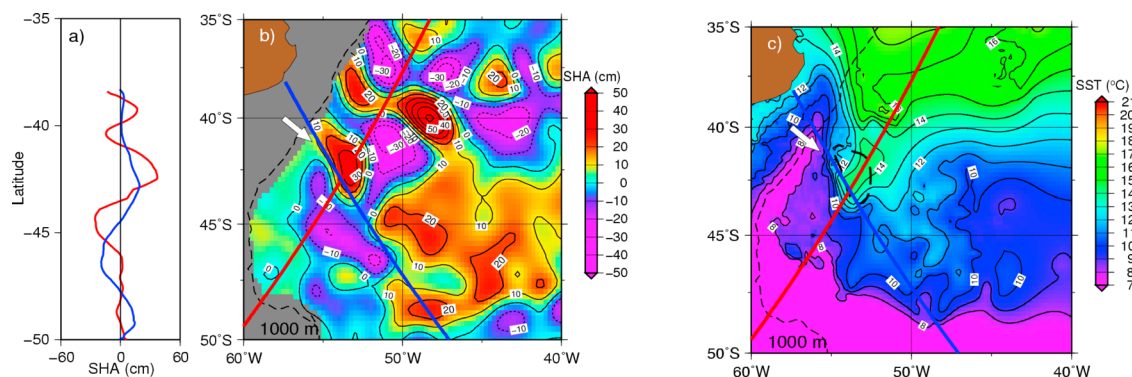
Figure 11. a) Along-track sea height anomaly (SHA) of ring TP-39-98 of 22 July 1998 for two altimeter ground tracks, (b) SHA field on the same date, and (c) sea surface temperature (SST) field on 21 July 1998. The arrows indicate the location of a Brazil Current ring.

53°W and 42.5°S. As in the previous description, the upper layer thickness fields indicate that the large values of sea height anomalies are representative of a Brazil Current ring and not of the Brazil Current front. The sea surface temperature field shows rather weak horizontal gradients of 0.013°C km^{-1}, but still clearly indicate the presence of a Brazil Current ring.

3.7. Brazil Current Transport and Ring Formation

[37] The aim of this section is to examine the hypothesis of the relative increase in the baroclinic transport of the Brazil Current and its association with anticyclonic ring shedding, as in the case of the Agulhas Current rings [*Goni et al.*, 1997]. This approach, similar to the one used by *Garzoli et al.* [1997] to monitor the upper-layer transport in the southeastern Atlantic, is computed across ground track *d*294 (Figure 12, top panel) using the altimetry-derived SHA values, climatology-derived estimates of ULT, and the reduced gravity field [*Goni and Wainer*, 2001, section 3).

[38] The time series of altimetry-derived southward baroclinic transport of the Brazil Current across *d*294 between 36°S and 38°S for the 6-year period and anticyclones lifetime is shown in Figure 12. Solid black circles (squares) indicate the times when rings are first detected in the ULT (SST) fields. The altimeter-derived baroclinic transport ranges from 2 to 42 Sv with a mean value of 16 ± 3 Sv for the 6-year time series, which is also consistent with transport values reported in the literature [*Gordon and Greengrove*, 1986; *Gordon*, 1989; *Garzoli and Garraffo*, 1989; *Zemba*, 1991; *Peterson*, 1992; *Garzoli*, 1993; *Mamaatuaiahutapu et al.*, 1998]. Mean annual baroclinic transport for each year are indicated by the horizontal lines (Figure 12, bottom panel). Results obtained here suggest a link between the baroclinic transport variability of the Brazil Current and ring shedding, as relatively moderate-to-high increments in the upper-layer transport of the Brazil Current are usually followed by the formation and shedding of anticyclonic rings. However, this relation falls short on three occasions (March 1993, August and October 1996), when a relative increase in the baroclinic transport is not followed by the shedding of a ring (Figure 12, bottom panel). This uncertainty may be partly due because some rings can not be identified when they are shed inside the diamond-shaped grid formed by the T/P ground tracks and/

or for not having a strong infrared surface signature. A comparison between ULT-derived (continuous line) rings and AVHRR (dashed line) observed rings is also shown in Figure 12 (middle panel). At any given time, two to three rings coexist in the region of study (Figure 12, shaded region in middle panel).

3.8. Comparison With Other Major Warm-Core Rings

[39] A comparison between the T/P-derived Brazil Current rings observed here and the characteristics of the most observed warm-core rings of other ocean basins is summarized in Tables 3 and 4. The origin of all these anticyclonic features are related to western boundary currents.

[40] Rings form directly from relatively strong ocean currents as a final product of an instability process [*Olson*, 1991]. However, ring formation mainly occurs in two different ways, depending on how the boundary currents separate from the coastline. For example, when the separation is smooth, as is the case for the Gulf Stream and Kuroshio currents, the current exhibits wave-like meanders that increase in amplitude toward the ocean interior. As these grow, there is a tendency for portions of the fluid to close off completely onto the parent current and a new ring is formed. In this case, newly formed rings pinch off in the downstream region and the current turns back into a more linear, zonal flow. On the other hand, when the boundary current overshoots its latitude of separation from the coastline and loops back onto itself, as is the case for the Brazil and East Australian currents, it forms a large, quasi-stationary meander near the coast with decreasing amplitude toward the ocean interior. Rings then detach from the first or second meander crest closer to the coast. Apart from these two different ring formation processes, the Agulhas Current can be considered as an interesting "hybrid" case, in the sense that the current runs out of its boundary prior to the wind stress maximum associated with typical latitudes of separation [*Olson*, 1991]. After it separates from the curved southern tip of the African continent, it retroflects, forming a large-amplitude lobe where anticyclonic rings are formed and released into the South Atlantic Ocean. Compared with other western boundary currents, the Agulhas Current exhibits a remarkable stability, with very little sideways meandering along most of its trajectory [*De Ruijter et al.*, 1999].
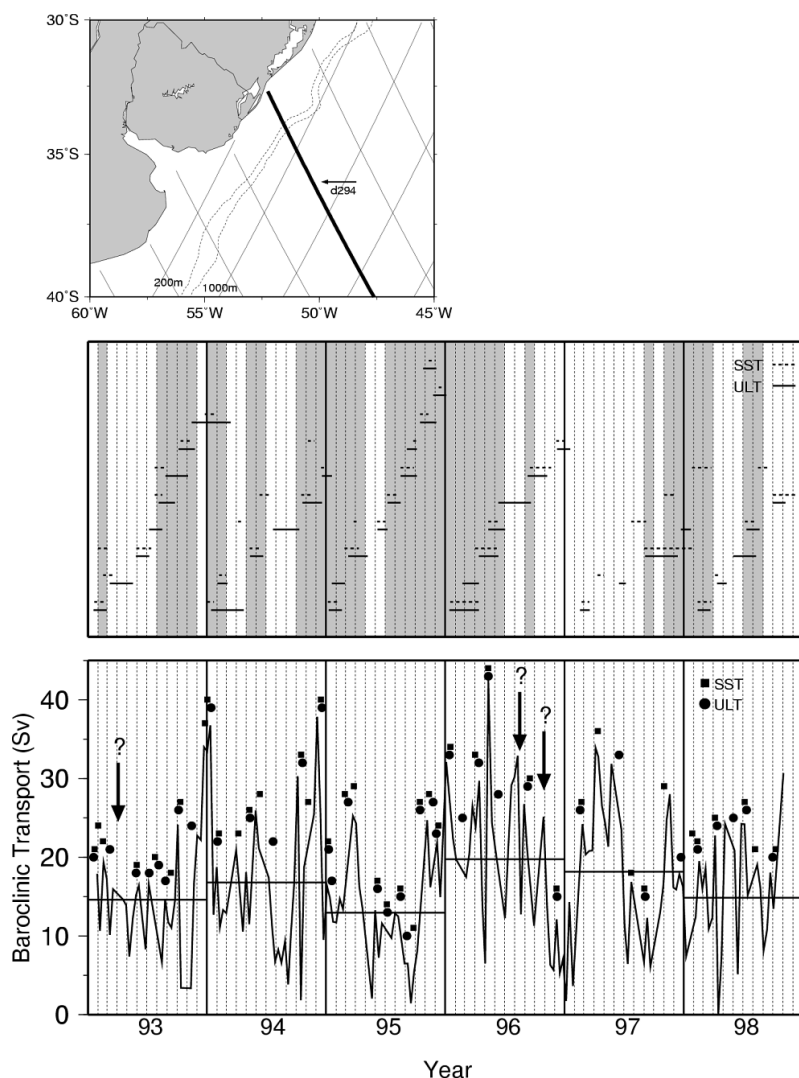
Figure 12. (top) TOPEX/Poseidon ground track *d*294 used to estimate the Brazil Current baroclinic transport. The 200-m and 1000-m isobaths are superimposed. (middle) Horizontal dashed lines indicate the lifetime of Brazil Current rings as obtained from sea surface temperature (SST) fields. Solid lines indicate lifetime obtained from upper layer thickness (ULT) fields. Shaded regions indicate when two or three rings coexist in the confluence region. (bottom) Time series of baroclinic transport across *d*294 derived from altimetry. Squares (circles) show the time of shedding as obtained from SST (ULT) fields. Horizontal lines indicate the annual mean of baroclinic transport. Three increases in baroclinic transport, indicated by a question mark, are not linked to a ring shedding event.

[41] The mean translation speed for Brazil Current rings obtained here was 9.8 ± 4.7 km y^{-1} (Table 1). On the other hand, Gulf Stream rings have a mean speed of 5 km d^{-1} [*Brown et al.*, 1986], up to 10 times faster than the speed expected for an equivalent upper layer isolated ring from theory [*Nof*, 1981; *Flierl*, 1984]. However, *Evans et al.* [1985] show that ring translation speed can be modulated up to 39 km d^{-1} depending on the presence or absence of external forcing. Advection by the large-scale mean circulation and interactions with the Gulf Stream are suggested to account for this difference.

[42] One important result from the compilation of the results shown in Tables 3 and 4 is that rings from these two types of formation and from various current systems are rather similar in their basic characteristics. Among the largest anticyclonic rings listed here, the Agulhas rings stand as being the most energetic and more linear than the others. Agulhas rings also have a low Rossby number ($R_o \sim 0.05$) and are at least twice as energetic as the Gulf of Mexico (GM) and North Brazil Current (NBC) rings. The NBC rings, which have almost the same horizontal length scale L as the Agulhas rings, are much more nonlinear (higher R_o) than the others [*Fratantoni et al.*, 1995]. The ULT-derived parameters computed in this study have the same order of magnitude with those reported by *Gordon* [1989], *Olson* [1991], and *Lentini et al.* [2002]. It is important to point out that the Gulf Stream, the Brazil Current and the Agulhas rings, form at approximately the same annual rate and more frequently than the Kuroshio rings (Table 4). As they move poleward, most of the rings

Table 3. Comparison Between Typical Warm-Core Rings of the World Oceans Based on Observations, Along With Mean Values Determined in This Study[a]

Location	g', m/s^2	L, km	R_d, km	Ro	APE, $\times10^{15}$J	h_1, m	Reference
Brazil	**0.014**	55	19	...	2.3	250	**this study**
Brazil	0.012	60	23	0.09	5.6	400	*Gordon* [1989]
GS	0.011	50	25	0.23	4.2	500	*Olson et al.* [1985]
GS	...	79	26	0.23	9.1	...	*Joyce* [1984]
Agulhas	0.018	123	44	0.06	41.0	500	*Olson and Evans* [1986]
Agulhas	0.013	80	30	0.06	11.3	690	*Duncombe Rae et al.* [1996]
Agulhas[b]	0.011	116	26	...	24	597	*Goni et al.* [1997]
Kuroshio	...	90	35	0.11	22.0	500	*Tomosada* [1978]
NBC	0.012	125	122	0.19	9.2	500	*Fratantoni et al.* [1995]
EA	...	85	30	0.14	14	...	*Nilsson and Cresswell* [1981]
GM	...	149	42	0.10	10	...	*Elliott* [1982]

[a]Mean values determined in this study are shown in first row in bold. Here g' is the reduced gravity, L is the radius of the ring, APE is the available potential energy, and h_1 is the upper layer thickness (ULT). R_d is the Rossby radius of deformation ($R_d = \frac{\left(g'h_1\right)^{1/2}}{f_0}$) and the nondimensional Rossby number, Ro, is $Ro = \frac{v_{max}}{f_0 L}$. (For our calculation, $Ro = \frac{g'\delta h_1}{f_0^2 L^2}$). For the NBC rings, $f_0 = 0.2 \times 10^{-4}$ s^{-1} instead of $f_0 = 1 \times 10^{-4}$ s^{-1}. Some numerical values were computed from the tabulations of *Olson* [1991], who, in turn, drew his values from the stated references. Abbreviations: GS, Gulf Stream; NBC, North Brazil Current; EA, Eastern Australian; and GM, Gulf of Mexico.

[b]Values were estimated applying the same methodology adopted in this study.

seem to disappear either by mixing or by coalescing with their parent current, except the Agulhas rings, which drift northwestward toward the subtropical gyre.

3.9. Heat Flux of Brazil Current Rings

[43] The heat anomaly contained in an anticyclonic ring is $Q = \rho_1 c_p \pi \Delta T h_0 L^2$, where ρ_1 is the mean density of the water, and c_p is the mean specific heat at constant pressure taken as 4000 J $°$C^{-1}m^{-1}. Considering that a typical Brazil Current ring has a mean radius (length scale) of 55 km, a mean vertical extension (h_0) of 160 m, a mean lifetime of approximately 2 months, and a mean temperature difference of $\Delta T \sim 5°$C between the inner core of the ring and the surface temperature of the surrounding waters outside its influence (Table 1), its heat anomaly is approximately 0.3×10^{20} J, which is equivalent to an intergyre heat flux of approximately 0.0065 PW per ring in the southwestern Atlantic region. Similar estimates of heat anomaly contained within the Agulhas rings of 2.4×10^{20} J [*van Ballegooyen et al.*, 1994], that correspond to an Agulhas heat flux of 0.0075 PW per ring, indicate that they are approximately eight times larger than the values estimated for Brazil Current rings. Assuming that, on average, the Brazil Current rings are shed into the southwestern Atlantic

at a rate of seven rings per year and that their mean life time is of 53 days, the heat flux anomaly relative to the South Atlantic thermocline waters is estimated to be approximately 0.045 PW per year. This amount of heat flux is equal to the mean annual value reported in the southeastern Atlantic [*van Ballegooyen et al.*, 1994] via the Agulhas ring field. However, this annual heat anomaly flux is almost twice the value previously reported by *Lentini et al.* [2002] using infrared imagery. This difference may be partly due to the discrepancies in the values of the parameters obtained using different observations and methodologies, which may reinforce the idea of combining two or more types of measurements to provide a more accurate statistics of the mesoscale field.

3.10. Fate of Brazil Current Rings

[44] Neither the fate of the southward propagating Brazil Current rings nor the role played by the reabsorbed rings in the adjacent environment is completely understood yet. While Brazil Current rings do not appear to be a major contributor of the net heat flux, in contrast to the case of the Agulhas rings, they may be important in regional water mass formation and modification. Although Brazil Current rings move mostly southward after detaching from the

Table 4. Characteristics of Warm-Core Rings of Five Current Systems of the World, Along With Values Determined From This Study[a]

Location	Frequency, Ring/Year	Predominant Movement	Disappearance,	Core Temperature $°$C	Reference
Brazil	**6−7**	**SW-SE**	**poleward coalesce mixing?**		**this study**
Brazil	6−7	SW-SE	poleward **coalesce mixing?**	~18	*Lentini et al.* [2002]
Brazil	6−?	S-SE	poleward and mixing	~14	*Gordon* [1989]
GS	8	SW	reabsorbed	~16	*Brown et al.* [1986] *Olson et al.* [1985]
Agulhas	7	W-NW	collide with Brazil Current	~17	*Duncombe Rae et al.* [1996] *Gordon and Haxby* [1990]
Kuroshio	1−2	poleward	poleward and mixing coalesce	~15	*Hata* [1974] *Tomosada* [1986]
EA	3	complex loops superimposed on poleward or equatorward drift	poleward and mixing coalesce	~19	*Nilsson and Cresswell* [1981]

[a]Values determined from this study are in bold. Some of the numerical values were taken from previous tabulations [*Tomosada*, 1986].

Brazil Current poleward excursions, most of them do not appear to be reabsorbed by their parent current as is the case of Gulf Stream rings [*Richardson*, 1980; *Brown et al.*, 1986]. From the ULT estimates, only four rings are reabsorbed by the Brazil Current subtropical front, whereas from AVHRR observations this number amounts to seven rings during the same period of time. *Legeckis and Gordon* [1982] and *Gordon* [1989] speculate that after winter, these southward-propagating rings may lose their surface signatures, eventually sink as they cool, and then reenter the subtropical gyre at subsurface depths.

[45] Evidence from other western boundary current regions suggests that rings are important sites for water mass modification and thermocline ventilation [*Tomosada*, 1978; *Schmitt and Olson*, 1985; *Gordon*, 1989; *Olson et al.*, 1992]. It is plausible that this process may result in deep winter mixed layers of mid- to sub-thermocline waters, some of which may be reentrained into the subtropical gyre [*Schmitt and Olson*, 1985; *Gordon*, 1989]. In the North Atlantic, the role of these relatively deep, winter-mixed pockets are associated with Subtropical Mode Water formation east of the Gulf Stream front, where the anticyclonic rings recoalesce with their parent current. In the southwestern Atlantic, *Gordon* [1981] observed a series of relatively warm and thick saline boluses at mid-thermocline depths (300–600 m) along 38°S. The author interpreted these as a consequence of surface convective processes, particularly during wintertime when cooling is strong. These subsurface relatively warm and anomalously saline layers may be an important source of salt for the transition zone between subtropical and subantarctic fronts [*Gordon et al.*, 1992; *Gordon*, 1989]. According to estimates by *Gordon* [1989], a 200 km-wide ring extending down to ∼400 m would be an important source of salt for the transition zone. Alternatively, if not all of the Brazil Current rings merge into the transition zone, the remaining winter-cooled rings may reenter and ventilate the South Atlantic thermocline after they rejoin the subtropical gyre [*Smythe-Wright et al.*, 1996], although the mechanisms involved are still unclear and need further investigation.

4. Summary and Conclusions

[46] TOPEX/Poseidon-derived sea height anomaly fields combined with climatological data within a two-layer reduced gravity scheme have been shown to be well suited to investigate the upper ocean dynamics and to identify and track mesoscale rings during the 6-year period (January 1993 to October 1998) in the southwestern Atlantic Ocean. Through an interpolation scheme, fields of sea height anomaly and upper layer thickness were obtained every 5 days to identify, track, and investigate the dynamics of 40 warm-core rings shed by the Brazil Current poleward extension during this period.

[47] On the basis of the upper layer fields, the Brazil Current rings were tracked off the southwestern Atlantic continental slope. The observed lifetime of Brazil Current rings ranged between 1 and 4 months, with a mean value of approximately 2 months. At any given time, two to three anticyclonic rings coexisted in the area of study. Most of the rings spawned at the confluence drifted southward without coalescing with the main thermocline. Only four rings were identified as being reabsorbed by the Brazil Current front after being shed. No evidence of propagation or absorption of Brazil Current rings into the eastern limb of the subtropical gyre was found.

[48] These rings, which are formed and released during the northward retreat of the Brazil Current, have a mean horizontal length scale of 55 km, mean upper layer thickness of 260 m, and mean translation speed of 10 km d^{-1}. The volume anomaly, which is determined by the maximum along-track depth of the ring measured relative to h_{∞} and by the length scale, L, has a mean value of 3.6×10^{12} m^3. Analysis of volume anomaly suggests that at least one "large" ring ($VOL \geq 3.6 \times 10^{12}$ m^3) is shed per year. Values computed for the available potential energy (*APE*) range from 0.01 to 9.1×10^{15} J, with a mean value of 2.5×10^{15} J.

[49] Ring formation seems to be linked to the Brazil Current southward baroclinic transport, estimated across the T/P ground track *d*294 between 36°–38°S, as relatively moderate-to-high increments in the upper-layer transport are usually followed by the formation and shedding of an anticyclone. If assumed that, on average, Brazil Current rings are shed in the Brazil-Malvinas Confluence region at a rate of seven rings per year, the flux of additional heat relative to the South Atlantic thermocline waters (relative to the 8° C isotherm) via the Brazil Current ring field is estimated to be approximately 0.045 PW per year. This is approximately the same value found for the Agulhas ring field by *van Ballegooyen et al.* [1994].

[50] In conclusion, despite a nonperfect match between ULT- and AVHRR-derived ring characteristics, the overall statistics seem to reflect quite well the properties of Brazil Current rings when compared to previous hydrographic and infrared observations. Although some uncertainties in ring identification and characterization have been found, the combination of these two different data sets proved to be an extremely useful tool to study mesoscale warm-core rings in an undersampled region, such as the southwestern Atlantic. It is important to notice that it is not always possible to compute the parameters of a ring from direct hydrographic data or thermal surface observations. Therefore the altimetry-derived data have been shown to be an excellent alternative in which SHA fields along with climatological data can provide a good proxy to estimate the physical properties of a ring. ULT fields are used for the first time to document statistics on spatial/temporal distribution, size, trajectory, translation velocity, volume anomaly, and available potential energy of Brazil Current rings in a continuous fashion.

[51] While the Brazil Current rings do not appear to be a major contributor to the meridional heat flux as in the case of the Agulhas rings, at least locally, they may be important in regional water mass formation and modification. The meridional heat anomaly flux estimates obtained here for the Brazil Current rings may also serve as a basis for regional model validation. In fact, the role played by these rings in the adjacent environment is still poorly understood and long-term monitoring programs are necessary to precisely assess the heat/salt and mass contribution of these rings to the southwestern Atlantic Ocean and to the large-scale deep flow. In addition, the dynamics of the Brazil and Malvinas western boundary currents and their interaction

with the large-scale upper circulation in the South Atlantic should be also scrutinized.

References

Bianchi, A. A., C. F. Giulivi, and A. R. Piola (1993), Mixing in the Brazil-Malvinas Confluence, *Deep Sea Res.*, 40, 1345–1358.

Brown, O. B., P. C. Cornillon, S. R. Emmerson, and H. M. Carle (1986), Gulf Stream warm rings: A statistical study of their behavior, *Deep Sea Res.*, 33, 1459–1473.

Byrne, D. A., A. L. Gordon, and W. F. Haxby (1995), Agulhas eddies: A synoptic view using Geosat ERM data, *J. Phys. Oceanogr.*, 25, 902–917.

Cheney, R., L. Miller, R. Argreen, N. Doyle, and J. Lillibridge (1994), TOPEX/Poseidon: The 2-cm solution, *J. Geophys. Res.*, 99, 24,555–24,564.

Conkright, M. E., et al. (1998), World Ocean Database 1998, *Internal Rep. 14*, 113 pp., Natl. Oceanogr. Data Cent., Silver Spring, Md.

De Ruijter, W. P. M., P. J. Van Leeuwen, and J. R. E. Lutjeharms (1999), Generation and evolution of Natal pulses: Solitary meanders in the Agulhas Current, *J. Phys. Oceanogr.*, 29, 3043–3055.

Dewar, W. K., and G. R. Flierl (1987), Some effects of the wind on rings, *J. Phys. Oceanogr.*, 17, 1653–1667.

Didden, N., and F. Schott (1993), Eddies in the North Brazil Current Retroflection region observed by Geosat altimetry, *J. Geophys. Res.*, 98, 20,121–20,131.

Duncombe Rae, C. M., S. L. Garzoli, and A. L. Gordon (1996), The eddy field of the southeast Atlantic Ocean: A statistical census from the Benguela sources and transports project, *J. Geophys. Res.*, 101, 11,949–11,964.

Elliott, B. A. (1982), Anticyclonic rings in the Gulf of Mexico, *J. Phys. Oceanogr.*, 12, 1292–1309.

Evans, R. H., K. S. Baker, O. B. Brown, and R. C. Smith (1985), Chronology of warm-core ring 82-B, *J. Geophys. Res.*, 90, 8803–8811.

Figueroa, D. E., J. M. D. de Astarloa, and P. Martos (1998), Mesopelagic fish distribution in the southwest Atlantic in relation to water masses, *Deep Sea Res., Part I*, 45, 317–332.

Flierl, G. R. (1984), Rossby wave radiation from a strongly nonlinear warm eddy, *J. Phys. Oceanogr.*, 14, 47–58.

Forbes, C., K. Leaman, D. B. Olson, and O. O. Brown (1993), Eddy and wave dynamics in the South Atlantic as diagnosed from GEOSAT altimeter data, *J. Geophys. Res.*, 98, 12,297–12,314.

Fratantoni, D. M., W. E. Johns, and T. L. Townsend (1995), Rings of the North Brazil Current: Their structures and behavior inferred from observations and a numerical simulation, *J. Geophys. Res.*, 100, 10,633–10,654.

Garzoli, S. L. (1993), Geostrophic velocity and transport variability in the Brazil-Malvinas Confluence, *Deep Sea Res., Part I*, 40, 1379–1403.

Garzoli, S. L., and A. Bianchi (1987), Time-space variability of the local dynamics of the Malvinas-Brazil confluence as revealed by inverted echo sounders, *J. Geophys. Res.*, 92, 1914–1922.

Garzoli, S. L., and Z. S. Garraffo (1989), Transports, frontal motions and eddies at the Brazil-Malvinas Currents Confluence, *Deep Sea Res.*, 36, 681–703.

Garzoli, S. L., G. J. Goni, A. J. Mariano, and D. B. Olson (1997), Monitoring the upper southeastern transports using altimeter data, *J. Mar. Res.*, 55, 453–481.

Goni, G. J., and I. Wainer (2001), Investigation of the Brazil Current front variability from altimeter data, *J. Geophys. Res.*, 106, 31,117–31,128.

Goni, G. J., S. Kalmholtz, S. L. Garzoli, and D. B. Olson (1996), Dynamics of the Brazil-Malvinas Confluence based upon inverted echo sounders and altimetry, *J. Geophys. Res.*, 101, 16,273–16,289.

Goni, G. J., S. L. Garzoli, A. Roubicek, D. B. Olson, and O. B. Brown (1997), Agulhas ring dynamics from TOPEX/Poseidon satellite altimeter data, *J. Mar. Res.*, 55, 861–883.

Gordon, A. L. (1981), South Atlantic thermocline ventilation, *Deep Sea Res.*, 28, 1239–1264.

Gordon, A. L. (1989), Brazil-Malvinas Confluence—1984, *Deep Sea Res.*, 36, 359–384.

Gordon, A. L., and C. L. Greengrove (1986), Geostrophic circulation of the Brazil-Falkland Confluence, *Deep Sea Res.*, 33, 573–585.

Gordon, A. L., and W. Haxby (1990), Agulhas eddies invade the South Atlantic: Evidence from GEOSAT altimeter and shipboard conductivity-temperature-depth survey, *J. Geophys. Res.*, 100, 3117–3125.

Gordon, A. L., R. F. Weiss, W. M. Smethie Jr., and M. J. Warner (1992), Thermocline and intermediate water communication between the South Atlantic and Indian oceans, *J. Geophys. Res.*, 97, 7223–7240.

Hata, K. (1974), Behavior of a warm eddy detached from the Kuroshio (in Japanese with English abstract), *J. Meteorol. Res.*, 26, 295–321.

Hooker, S. B., and J. W. Brown (1996), Dipole rings and vortex interactions of the Brazil Current, *IEEE Trans. Geosci. Remote Sens.*, 34, 1323–1330.

Houry, S., E. Dombrowsky, P. De Mey, and J.-F. Minster (1987), Brunt–Väisäla frequency and Rossby radii in the South Atlantic, *J. Phys. Oceanogr.*, 17, 1619–1626.

Joyce, T. M. (1984), Velocity and hydrographic structure of a Gulf Stream warm-core ring, *J. Phys. Oceanogr.*, 14, 936–947.

Joyce, T. M., and M. A. Kennelly (1985), Upper-ocean velocity structure of Gulf Stream warm-core ring 82-B, *J. Geophys. Res.*, 90, 8839–8844.

Legeckis, R., and A. L. Gordon (1982), Satellite observations of the Brazil and Falkland currents—1975 to 1976 and 1978, *Deep Sea Res.*, 29, 375–401.

Lentini, C. A. D., G. P. Podestá, and E. J. D. Campos (2000), The annual cycle of satellite-derived sea surface temperature on the western South Atlantic shelf, *Rev. Bras. Oceanogr.*, 48, 93–105.

Lentini, C. A. D., G. P. Podestá, E. J. D. Campos, and D. B. Olson (2001), Sea surface temperature anomalies in the western South Atlantic from 1982 to 1994, *Cont. Shelf Res.*, 21, 89–112.

Lentini, C. A. D., D. B. Olson, and G. P. Podestá (2002), Statistics of Brazil Current rings observed from AVHRR: 1993 to 1998, *Geophys. Res. Lett.*, 29(16), 1811, doi:10.1029/2002GL015221.

Mamaatuaiahutapu, K., V. Garçon, C. Provost, and H. Mercier (1998), Transports of the Brazil and Malvinas currents at their confluence, *J. Mar. Res.*, 56, 417–438.

Mariano, A. J., and O. B. Brown (1992), Efficient objective analysis of dynamically heterogeneous and nonstationary fields via the parameter matrix, *Deep Sea Res.*, 39, 1255–1271.

McDonagh, E. L., and K. J. Heywood (1999), The origin of an anomalous ring in the southeast Atlantic, *J. Phys. Oceanogr.*, 29, 2025–2064.

Mellor, G. L., C. R. Mechoso, and E. Keto (1982), A diagnostic calculation of the general circulation of the Atlantic Ocean, *Deep Sea Res.*, 29, 1171–1192.

Mied, R. P. (1989), The decay of mesoscale vortices, in *Mesoscale/Synoptic Coherent Structures in Geophysical Turbulence, Oceanogr. Ser.*, vol. 50, edited by J. C. J. Nihoul and B. M. Jamart, pp. 135–147, Elsevier, New York.

Nilsson, C. S., and G. R. Cresswell (1981), The formation and evolution of East Australian Current warm-core eddies, *Prog. Oceanogr.*, 9, 133–183.

Nof, D. (1981), On the β-induced movement of isolated baroclinic eddies, *J. Phys. Oceanogr.*, 11, 1662–1672.

Okada, Y., and Y. Sugimori (1986), Decay of warm-core rings based on observations of available potential energy, *Deep Sea Res.*, 33, 1577–1599.

Olson, D. B. (1986), Lateral exchange within Gulf Stream warm-core ring surface layers, *Deep Sea Res.*, 33, 1692–1704.

Olson, D. B. (1991), Rings in the ocean, *Annu. Rev. Earth Planet. Sci.*, 19, 283–311.

Olson, D. B., and R. H. Evans (1986), Rings of the Agulhas Current, *Deep-Sea Res.*, 33, 27–42.

Olson, D. B., R. W. Schmitt, M. A. Kennelly, and T. M. Joyce (1985), A two-layer diagnostic model of the long term physical evolution of warm-core ring 82-B, *J. Geophys. Res.*, 90, 8813–8822.

Olson, D. B., G. P. Podestá, R. H. Evans, and O. B. Brown (1988), Temporal variations in the separation of Brazil and Malvinas Currents, *Deep Sea Res.*, 35, 1971–1990.

Olson, D. B., R. A. Fine, and A. L. Gordon (1992), Convective modifications of water masses in the Agulhas, *Deep Sea Res.*, 39, S163–S181.

Peterson, R. G. (1992), The boundary currents in the western Argentine Basin, *Deep Sea Res.*, 39, 623–644.

Richardson, P. L. (1980), Gulf Stream ring trajectories, *J. Phys. Oceanogr.*, 10, 90–104.

Schmitt, R. W., and D. B. Olson (1985), Wintertime convection in warm core rings: Thermocline ventilation and the formation of mesoscale lenses, *J. Geophys. Res.*, 90, 8823–8838.

Smythe-Wright, D., A. L. Gordon, P. Chapman, and M. S. Jones (1996), CFC-113 shows Brazil eddy crossing the South Atlantic to the Agulhas retroflection region, *J. Geophys. Res.*, 101, 885–895.

Tomosada, A. (1978), Oceanographic characteristics of a warm eddy detached from the Kuroshio east of Honshu, *Jpn. Bull. Tokai Reg. Fish. Res. Lab.*, 94, 59–103.

Tomosada, A. (1986), Generation and decay of Kuroshio warm-core rings, *Deep Sea Res.*, *33*, 1475–1486.

van Ballegooyen, R. C., M. L. Grundlingh, and J. R. E. Lutjeharms (1994), Eddy fluxes of heat and salt from the southwest Indian Ocean into the southeast Atlantic Ocean: A case study, *J. Geophys. Res.*, *99*, 14,053–14,070.

Vigan, X., C. Provost, and G. P. Podestá (2000), Sea surface velocities from sea surface temperature image sequences: 2. Application to the Brazil Malvinas Confluence area, *J. Geophys. Res.*, *105*, 19,515–19,534.

Vivier, F., and C. Provost (1999), Volume transport of the Malvinas Current: Can the flow be monitored by TOPEX/Poseidon?, *J. Geophys. Res.*, *104*, 21,105–21,122.

Vukovich, F. M., and G. A. Maul (1985), Cyclonic eddies in the eastern Gulf of Mexico, *J. Phys. Oceanogr.*, *15*, 105–117.

Zemba, J. C. (1991), The structure and transport of the Brazil Current between 27 and 36 south, Ph.D. thesis, Mass. Inst. of Technol./Woods Hole Oceanogr. Inst., Woods Hole, Mass.

G. J. Goni, Physical Oceanography Division, Atlantic Oceanographic and Meteorological Laboratory, NOAA, U. S. Department of Commerce, 4301 Rickenbacker Causeway, Miami, FL 33149, USA. (gustavo.goni@noaa.gov)

C. A. D. Lentini, Instituto Oceanográfico, Universidade de São Paulo, Praça do Oceanográfico, 191, 05508-900 Sao Paulo, SP, Brazil. (lentini@io.usp.br)

D. B. Olson, Division of Meteorology and Physical Oceanography, Rosenstiel School of Marine and Atmospheric Science, University of Miami, 4600 Rickenbacker Causeway, Miami, FL 33149-1098, USA.